*FUDMA Journal of Sciences (FJS)*
*ISSN: 2616-1370*
*Vol. 2 No. 2, June, 2018, pp 116 - 132*

# THERMAL AND VELOCITY SLIP EFFECTS ON HEAT AND MASS TRANSFER OF A HYDROMAGNETIC MAXWELL FLUID FLOW OVER A STRETCHING SHEET

**[1]Baoku, I.G. and [2]Onifade, Y. S.**

[1]Department of Mathematical Sciences, Federal University, Dutsin-Ma, Katsina State, Nigeria.
[2]Department of Physics, Federal University of Petroleum Resources, Effurun, Delta State, Nigeria.

Corresponding Author E-mail: ibaoku@fudutsinma.edu.ng

**ABSTRACT**
In the present study, the effects of thermal and velocity slip on steady boundary layer magnetohydrodynamic flow, heat and mass transfer of an incompressible upper convected Maxwell fluid over a permeable stretching sheet are analyzed. Similarity transformation technique is adopted to obtain the self-similar coupled nonlinear ordinary differential equations and then the self-similar equations are solved numerically using Runge-Kutta-Fehlberg integration technique with shooting method. The velocity and temperature fields are enhanced by increasing values of velocity and thermal slip parameters respectively. The wall shear stress, rates of heat and mass transfer are enhanced by the increments in the values of thermal and velocity slip parameters. The presence of thermal and velocity slip on the flow fields is found to be of great significance to the investigation.

***Keywords****: Velocity slip, Thermal slip, Maxwell fluid, Hydromagnetic flow, Heat and mass transfer, Stretching sheet.*

## INTRODUCTION

Mechanics of non-Newtonian fluids has emerged as one of the most important research areas of modern Applied Mathematics. Many biological and industrial fluids have elastic characteristics which cannot be ignored because most of them are suspensions of particles in the viscous liquid with short memory. As a result of this, almost all biological and industrial fluids are non-Newtonian for which the Navier-Stokes equations are inadequate. Such fluids are found to exhibit a non-linear stress strain relation and thus the resulting differential systems of equations are highly nonlinear. Keeping these challenges in view, many investigators have engaged in obtaining solutions for flow, heat and mass transfer of non-Newtonian fluid with different geometries. For these, one may refer to the studies of Sarpakaya (1961), Soundalgekar (1974), Gupta and Sridhar (1985), Anderson (1992), Eldabe-Nabil and Mohammed-Mona (2002), Vajravelu and Rollins (2004), Khan and Sanjayanand (2005), Sanjayanand and Khan (2006), Abel and Mahesha (2008), Prasad *et al.* (2010), Olajuwon and Baoku (2014), Baoku and Olajuwon (2014), Baoku (2014), Baoku *et al.* (2015), Koriko *et al.* (2016), Popoola *et al.* (2016) and Rahbari *et al.* (2018).

Generally, non-Newtonian fluids are categorized into three types, namely; the differential, rate and integral types. The simplest class of rate type fluid is known as Maxwell fluid. Maxwell fluid model is important especially to viscoelastic problems having small dimensionless relaxation time. The problems of hydrodynamic Sakiadis flow of an upper-convected Maxwell (UCM) fluid over a rigid plate moving steadily in a quiescent fluid was investigated by Sadeghy *et al.* (2005). They employed perturbation method and two numerical schemes, namely; the Runge-Kutta and finite difference methods for the solution to the problem. Hayat and Sajid (2006) extended the work of Sadeghy *et al.* (2005) to magnetohydrodynamic flow for the totally analytic solution of the problem. Fetecau and Fetecau (2003a,b,c) examined the problems of Maxwell fluids past an infinite plate; on the Rayleigh-Stokes problems; and on decay of a potential vortex respectively. Zierep and Fetecau (2007) further studied the Rayleigh-Stokes problem of a Maxwell fluid for three different types of initial and/or boundary conditions. Hayat *et al.* (2008) also discussed the magnetohydrodynamic (MHD) flow and mass transfer of upper-convected Maxwell fluid past a porous shrinking sheet in the presence of chemically reactive species. Hayat and Qasim (2010) further provided solutions to the flow and mass transfer characteristics in a Maxwell fluid past a stretching sheet with Ohmic dissipation, thermal radiation and thermophoresis. Wang and Tan (2008) addressed the

stability analysis of double-diffusive convection of a Maxwell fluid in a porous medium.

Recently, Ishak *et al.* (2015) examined the effect of magnetohydrodynamic flow and heat transfer of the upper-convected Maxwell fluid over a stretching/shrinking sheet with prescribed heat flux. They obtained numerical solution for their problem. Mustapha *et al.* (2015) also addressed a steady flow of Maxwell nanofluid induced by an exponentially stretching sheet subject to convective heating. Numerical solutions were obtained for the emerging non-linear boundary value problem using MATLAB built-in function bvp4c. They concluded that velocity decreases and temperature increases when the local Deborah number is increased. Hayat *et al.* (2015) investigated the convective heat and mass transfer of a three-dimensional flow of Maxwell fluid over a stretching surface with heat source. Concentration and thermal buoyancy effects were accounted for and concentration boundary layer thicknesses were found to be decreasing functions of stretching ratio. Omowaye and Animasaun (2016) analyzed the upper convected Maxwell fluid flow in variable thermophysical properties over a melting surface situated in hot environment subject to thermal stratification. They concluded that an increase in stratification parameter corresponds to decrease in the heat energy entering into the fluid domain from free stream and this significantly reduces the overall temperature and temperature gradient of UCM fluid as it flows over a melting surface.

Adegbie *et al.* (2015) presented the dynamics of an upper-convected Maxwell fluid flow with heat and mass transfer over a melting surface. They accounted for the influence of melting heat transfer, thermal and solution stratification in their work using the classical Runge-Kutta method with shooting technique. Mushtaq *et al.* (2014) took into account the influence of thermal radiation of the laminar two-dimensional incompressible stagnation point flow of an upper-convected Maxwell fluid over a stretching sheet. They investigated an entirely different aspect of Rosseland approximation for thermal radiation. Shateyi *et al.* (2015) explored spectral relaxation method to investigate the entropy generation on a flow and heat transfer of a Maxwell fluid. Pop *et al.* (2012) analyzed the MHD flow and heat transfer of an upper-convected Maxwell fluid over a stretching surface with variable thermophysical properties. Koriko *et al.* (2016) examined the boundary layer of an upper-convected Maxwell fluid flow with variable thermal-physical properties over a melting thermally stratified surface. They employed the classical Runge-Kutta method with shooting technique to find that the transverse velocity, longitudinal velocity and temperature of the UCM fluid were increasing functions of temperature-dependent viscous and thermal conductivity parameters.

Literature survey reveals that little attention has been paid to the slip flow, heat and mass transfer of non-Newtonian fluids especially Maxwell fluid. Fluid patterns characterized by the slip boundary conditions have special significances in many applications. In some instances, the fluids present a loss of adhesion at the wetted wall which compels it to slide along the wall. Consideration for no slip condition seems unrealistic for many non-Newtonian flows because they exhibit macroscopic wall slip. Particularly, no-slip condition is inadequate for rough surfaces and in micro electromechanical system (MEMS). The fluid which exhibits boundary slip finds applications in technology such as in the polishing of artificial heart and internal cavities in a variety of manufactured parts is achieved by imbedding such as fluids as abrasive [Sajid *et al.* (2008)].

In all the aforementioned investigations, the effects of slip conditions have not been taken into account for Maxwell fluids. Such effects are very important for non-Newtonian viscoelastic Maxwell fluid like polymer melts which exhibit wall slip. Hayat *et al.* (2010) studied the slip effects on the magnetohydrodynamic peristaltic flow of a Maxwell fluid in a planar channel saturated with porous medium. Vieru and Zafar (2013) discussed the Couette flows of a Maxwell fluid produced by the motion of a flat plate. They analyzed the flow with the assumption that the relative velocity between the fluid at the wall and the wall is proportional to the shear rate at the wall under the slip condition at boundaries. They obtained velocity fields corresponding to both slip and non slip conditions for Maxwell and Newtonian fluids. The slip flow rate of a non-Newtonian Maxwell fluid past a stretching sheet was investigated by Sajid *et al.* (2014). Liu and Guo (2017) recently examined the magnetohydrodynamic flow of a generalized Maxwell fluid induced by a moving plate where the second-order slip between the wall and the fluid was considered. They concluded that the velocity corresponding to flows with slip condition is lower than for flow with nonslip conditions, and the velocity with second-order slip condition is lower than that with first-order slip condition.

In this work, the steady laminar magnetohydrodynamic flow with velocity slip, mass and heat transfer with thermal slip in a Maxwell fluid over a porous stretching sheet is examined. To the best of the authors' knowledge, the detailed survey of literature shows that no attention has given to the combined effects of thermal and velocity slip on hydromagnetic flow of viscoelastic Maxwell fluid, heat and mass transfer over a permeable stretching surface. The mathematical model is proposed in the form of partial differential

equations. Similarity transformation is applied to convert the equations into dimensionless forms of ordinary differential equations. Numerical solution is sought using the Runge-Kutta-Fehlberg integration scheme with shooting technique. The numerical integrations are performed over a substantially large domain to satisfy the outer boundary layer conditions and a satisfactory convergence criterion is ensured in all cases. Physical quantities are analyzed against the varying emerging parameters using graphs and tables.

**MATHEMATICAL MODEL**

Consider a two-dimensional steady and incompressible boundary layer flow of an upper-convected Maxwell fluid over a stretching sheet with surface temperature $T_w$ and species concentration $C_w$. The stretching velocity of the sheet is $u_w = bx$ with $b$ being a constant. Let the wall constant mass transfer be $V_w$ with $V_w > 0$ for injection and $V_w < 0$ for suction where $V_w$ will be determined later. The flow is presumed to be generated by stretching sheet issuing from a thin slit at the origin. The sheet is then stretched in such a way that the speed at any point on the sheet becomes proportional to the distance from the origin. The respective free stream temperature and species concentration are $T_\infty$ and $C_\infty$. The coordinate system $x$ - axis is along the stretching sheet while $y$ - axis is normal to the sheet. The flow is subjected to a transverse and uniform magnetic field of strength $B_0$, which is applied in the positive $y$ - direction, normal to the surface. The induced magnetic field is assumed to be very small in comparison to the applied magnetic field. The chemical reaction is also presumed to occur over the surface but not in the fluid. Based on these assumptions and following Sadeghy *et al.* (2005) and Hayat and Sajid (2007), the governing equations of the conservation of mass, momentum, energy and species concentration, using an order magnitude analysis of the y-direction momentum equation (normal to the sheet) and the usual boundary layer assumptions with negligible pressure gradient where other thermophysical properties are kept as constants in the presence of magnetic field, past a stretching sheet can be expressed as follows:

$$\frac{\partial u}{\partial x} + \frac{\partial v}{\partial y} = 0 \tag{1}$$

$$u\frac{\partial u}{\partial x} + v\frac{\partial u}{\partial y} = \upsilon\frac{\partial^2 u}{\partial y^2} - \frac{\sigma B_0^2 u}{\rho} - k_0\left[v^2\frac{\partial^2 u}{\partial y^2} + 2uv\frac{\partial^2 u}{\partial x \partial y} + u^2\frac{\partial^2 u}{\partial x^2}\right] = 0 \tag{2}$$

$$\rho C_p\left(u\frac{\partial T}{\partial x} + v\frac{\partial T}{\partial y}\right) = \kappa\frac{\partial^2 T}{\partial y^2} \tag{3}$$

$$u\frac{\partial C}{\partial x} + v\frac{\partial C}{\partial y} = D_m\frac{\partial^2 C}{\partial y^2} \tag{4}$$

where $x$, $y$, $u$, $v$, $T$, $C$, $\upsilon$, $k_0$, $\sigma$, $B_0$, $\rho$, $C_p$, $\kappa$ and $D_m$ are coordinate axes along the continuous surface in the direction of motion and normal to it, velocity components in the directions of $x$ and $y$ axes, fluid temperature inside the boundary layer, species concentration of the fluid, kinematic viscosity, relaxation time, electrical conductivity, magnetic field flux, fluid density, specific heat at constant pressure, thermal conductivity and mass diffusivity respectively.

The boundary conditions for the problem are:

$$u = u_w + M\left(\frac{\partial u}{\partial y}\right), \qquad v = V_w, \quad T = T_w + N\frac{\partial T}{\partial y}, \qquad C = C_w \quad \text{at } y = 0 \tag{5}$$

$$u \to U_\infty = 0, \qquad T \to T_\infty, \qquad C \to C_\infty \qquad \text{as} \qquad y \to \infty \tag{6}$$

where $u_w = bx$, $T = T_w + d\left(\frac{x}{l}\right)^2$, $l$, $d$, $M$ and $N$ are the reference length of the sheet, a constant, velocity and thermal slip factors respectively. It should be noted that $M = N = 0$ corresponds to no-slip condition. The above boundary condition is valid when $x \ll l$ which occurs very near to the slit.

Introducing the following dimensionless quantities, the mathematical analysis of the problem is simplified by using the following similarity transforms:

$$\eta = \sqrt{\frac{a}{\upsilon}}y,\ \psi = \sqrt{a\upsilon}\, x f(\eta),\ \theta(\eta) = \frac{T - T_\infty}{T_w - T_\infty},\ \phi(\eta) = \frac{C - C_\infty}{C_w - C_\infty} \tag{7}$$

The continuity equation (1) is satisfied if a stream function $\psi = (x, y)$ is chosen as:

$$u = \frac{\partial \psi}{\partial y}\ ,\qquad v = -\frac{\partial \psi}{\partial x} \tag{8}$$

Using the above similarity transformation quantities, the governing equations (2) - (4) are transformed to the following coupled nonlinear ordinary differential equations:

$$K\left[2ff'f'' - f^2 f'''\right] + f''' + ff'' - \left(f' + Mn\right)f' = 0 \tag{9}$$

$$\theta'' + \Pr f\,\theta' = 0 \tag{10}$$

$$\phi'' + Sc\, f\,\phi' = 0 \tag{11}$$

with boundary conditions:

$$f(0) = S,\ f'(0) = \alpha + Af''(0),\ \theta(0) = 1 + B\theta'(0),\ \phi(0) = 1 \text{ at } \eta = 0 \tag{12}$$

$$f'(\infty) \to 0,\ \theta(\infty) \to 0,\ \phi(\infty) \to 0 \quad \text{as } \eta \to \infty \tag{13}$$

where the parameters are defined as:

$K = k_0 a$ is the Deborah number, $\eta$ is the similarity variable, prime is the differentiation with respect to $\eta$, $f'$, $\theta$ and $\phi$ are the dimensionless velocity, temperature and species concentration respectively, $Mn = \frac{\sigma \beta_0^2}{a\rho}$ is the magnetic interaction parameter, $\Pr = \frac{\mu C_p}{\kappa}$ is the Prandtl number, $Sc = \frac{\upsilon}{D_m}$ is the Schmidt number, $S = \frac{-V_w}{\sqrt{a\upsilon}}$ is the suction parameter, $\alpha = \frac{b}{a}$ is the stretching parameter, $A = M\left(\frac{a}{\upsilon}\right)^{\frac{1}{2}}$ is the velocity slip parameter and $B = N\left(\frac{a}{\upsilon}\right)^{\frac{1}{2}}$ is the thermal slip parameter.

Other important physical quantities of interest which are germane to the technological and engineering applications of the problem are the skin friction coefficient $C_f$, Nusselt number $Nu_x$ and Sherwood number $Sh_x$ which are defined as follows:

$$C_f = \frac{\tau_w}{\rho u_w^2},\quad Nu_x = \frac{x q_w}{\kappa(T_w - T_\infty)},\quad Sh_x = \frac{x h_w}{D_m(C_w - C_\infty)} \tag{14}$$

where the wall shear stress $\tau_w$, heat flux $q_w$ and mass flux $h_w$ are given by:

$$C_f\sqrt{\mathrm{Re}_x} = (1 + K)f''(0),\qquad \frac{Nu_x}{\sqrt{\mathrm{Re}_x}} = -\theta'(0),\qquad \frac{Sh_x}{\sqrt{\mathrm{Re}_x}} = -\phi'(0) \tag{15}$$

and $\mathrm{Re}_x = \frac{x u_w(x)}{\upsilon}$ is the local Reynolds number.

**NUMERICAL PROCEDURE**

An efficient fourth-fifth order Runge-Kutta-Fehlberg method alongside the shooting technique has been employed to investigate the flow model for the above coupled nonlinear ordinary differential equations (9) - (11) with mixed boundary conditions in equations (12) and (13) for different values of emerging parameter, namely: Deborah Number K, magnetic interaction parameter $Mn$, Prandtl number $\Pr$, Schmidt number $Sc$, velocity slip parameter $A$ and thermal slip parameter $B$. The nonlinear differential equations (9) – (11) are first decomposed into a system of first order differential equations. The coupled ordinary differential equations (9) - (11) are third order in $f(\eta)$ and second order in $\theta(\eta)$ and $\phi(\eta)$ which have been reduced to a system of seven simultaneous equations for seven unknowns. To numerically solve this system of equations using Runge-Kutta-Fehlberg method, the solutions require seven initial boundary conditions in all but two initial conditions in $f(\eta)$, one initial condition in each $\theta(\eta)$ and $\phi(\eta)$ are available. However, the values of $f'(\eta)$, $\theta(\eta)$ and $\phi(\eta)$ are known at $\eta \to \infty$. These free stream conditions are utilized to produce unknown initial conditions at $\eta = 0$ by employing shooting technique. The most important of this algorithm is to choose the appropriate The equations (9) – (11) can be expressed as:

$$f''' = \frac{1}{\left(1 - Kf^2\right)}\left[f'^2 - ff'' - 2Kff'f'' + Mnf'\right] \tag{16}$$

$$\theta'' = -\Pr f\,\theta' \tag{17}$$

$$\phi'' = -Sc\, f\,\phi' \tag{18}$$

The following new variables can be defined for the following equations:

$$f_1 = f(\eta),\ f_2 = f'(\eta),\ f_3 = f''(\eta),\ f_4 = \theta(\eta),\ f_5 = \theta'(\eta),\ f_6 = \theta(\eta),\ f_7 = \theta'(\eta) \tag{19}$$

The coupled higher order nonlinear differential equations and the mixed boundary conditions are transformed to seven equivalent first-order differential equations as follows:

finite value of $\eta_\infty$. Therefore, in order to estimate the value of $\eta_\infty$, some initial guess values are started with and the boundary value problems consisting of equations (9) - (11) are solved to obtain $f''(0)$, $\theta'(0)$ and $\phi'(0)$. The solution is repeated with another larger value of $\eta_\infty$ until two successive values of $f''(0)$, $\theta'(0)$ and $\phi'(0)$ differ only after the desired significant digit. The last value $\eta_\infty$ is taken as the finite value of the limit $\eta_\infty$ for the particular set of physical parameters for determining the velocity, temperature and the species concentration, which are respectively $f'(\eta)$, $\theta(\eta)$ and $\phi(\eta)$ in the boundary layer. After getting all the initial conditions, this system of simultaneous equations is solved using the fourth-fifth order Runge-Kutta-Fehlberg integration scheme. The value of $\eta_\infty = 10$ has been selected to be appropriate in nearly all cases for the physical parameters governing the flow. Thus, the coupled boundary value problem of third order in $f(\eta)$, second order in $\theta(\eta)$ and $\phi(\eta)$ has been reduced to a system of seven simultaneous equations of first order for seven unknown variables as follow:

$$\left.\begin{aligned} f_1' &= f_2 \\ f_2' &= f_3 \\ f_3' &= \frac{\left(f_2^{\,2} - f_1 f_3 - 2K f_1 f_2 f_3 + Mn f_2\right)}{\left(1 - K f_1^{\,2}\right)} \\ f_4^1 &= f_5 \\ f_5^1 &= -\Pr\, f_1 f_5 \\ f_6^1 &= f_7 \\ f_7^1 &= -Sc f_1 f_7 \end{aligned}\right\} \qquad (20)$$

Also, the boundary conditions are transformed as:

$$\left.\begin{aligned} &f_1(0) = S,\ f_2(0) = \beta + A f_3(0),\ f_4(0) = 1 + B f_5(0)\ ,\ f_6(0) = 1 \\ &f_2(\infty) = 0,\ f_4(\infty) = 0,\ f_6(\infty) = 0 \end{aligned}\right\} \qquad (21)$$

Hence, the boundary value problem in equations (9) – (11) with the boundary conditions (12) and (13) is now converted into an initial value problem in equation (20) with the initial conditions in equation (21). Then, the initial value problem is solved by employing Runge-Kutta-Fehlberg integrating scheme appropriately guessing the missing initial values using the shooting method. For several sets of emerging parameters, the step size of $\Delta\eta = 0.001$ is used for the computational purposes by translating the algorithm into MAPLE codes as described by Heck (2003) and error tolerance of $10^{-7}$ is used in all the cases. The results obtained are presented through plots for velocity, temperature and species concentration fields and through tables for local skin-friction coefficient, Nusselt and Sherwood numbers.

**DISCUSSION OF RESULTS**

The numerical solutions are obtained for the velocity, temperature and species concentration fields for different values of governing parameters. The results are displayed through graphs in Figures 1-16. It should be pointed out that Figures (1) - (5) satisfy the specified boundary conditions and Figures (6) - (16) reveal that the far field boundary conditions are satisfied asymptotically and hence this supports the accuracy of the numerical computations and results. Moreover, the behaviour of local skin friction coefficient, Nusselt number and Sherwood number due to the variations in various emerging parameters is also deliberated in Table 2. Table 1 depicts a comparison with previously published work of Hayat *et al.* (2011) available in the literature, in order to further check the accuracy of the present results.

The velocity field $f'$ for different values of Deborah number $K$, magnetic interaction parameter $Mn$, stretching parameter $\alpha$, suction parameter $S$ and velocity slip parameter $A$ are shown in Figures 1-5 respectively. Figure 1 reveals the influence of $K$ on the flow field. It is evident from this figure that $f'$ is a decreasing function of $K$. This implies that a decrease in the fluid velocity corresponds to an enhancement of the velocity boundary layer thickness. From the physical point of view, when shear stress is eliminated, the fluid will come to rest. This kind of phenomenon is experienced in many polymeric liquids that cannot be

defined in the viscous fluid model. Higher values of $K$ will produce a retarding force between two adjacent layers in the flow. For this reason, there will be a reduction in the velocity field and corresponding associated effect is noticed in the boundary layer thickness. Figure 2 shows the effect of $Mn$ on $f'$. It is obvious that an increase in the values of $Mn$ decrease the boundary layer thickness in the flow field. Figures 3 and 4 display the distinction of velocity field with respect to the variation in suction parameter $S$ and stretching parameter $\alpha$. On observing these figures, as the values of $S$ increases, the velocity field decreases as anticipated. However, the velocity field increases as the values of $\alpha$ increase. In the same manner, Figure 5 establishes that the velocity distribution is seen to increase with the increase in the values of $A$, thereby decreasing the boundary layer thickness.

Figures 6 - 11 illustrate the variations of $\theta$ with respect to $\eta$ for various values of $K$, $Mn$, $\alpha$, $\Pr$, $B$ and $S$ respectively. From Figures 6 and 7, it is observed that $K$ and $Mn$ have opposite effects on $\theta$. An increase in $K$ corresponds to an increment in the fluid temperature whereas the result of increasing $Mn$ reduces the thermal boundary layer thickness in the flow field. The thermal boundary layers also decrease as the values of $\alpha$ and $\Pr$ increase as displayed in Figures 8 and 9. Higher estimation of $\Pr$ is found to decay the temperature field. This is due to the fact that $\Pr$ expresses the ratio of momentum diffusivity to thermal diffusivity. Thus, small values of $\Pr$ implies that the thermal diffusivity dominates and for higher estimation of $\Pr$, the momentum diffusivity dominates. As the values of suction parameter $S$ increase, the temperature field decreases as shown in Figure 10. Consequently, the thermal boundary layer thickness and the surface temperature are also decreasing. Figure 11 demonstrates the variation of temperature with thermal slip parameter $B$. $B$ is found to enhance the thermal boundary layer thickness.

Figures 12 - 16 describe the effects of $K$, $Mn$, $S$, $\alpha$ and $Sc$ on the species concentration field. Figure 12 captures the influence of $K$ on the species concentration distribution. As expected, it is observed that for any given value of $\eta$, the species concentration becomes increased with an increase in $K$. The variation of $\phi$ with different values of $Mn$ is indicated by Figure 13. It is clear that the magnetic interaction parameter decreases the species concentration field. In Figures 14 and 15, it is interesting to note that $S$ and $\alpha$ have the same effects on the species concentration boundary layer. Both of them noticeably decrease the concentration layer thicknesses. Figure 16 is plotted to display the influence of $Sc$, which is the ratio of momentum diffusivity to mass diffusivity, on species concentration field. It is observed that increasing the values of $Sc$ corresponds to a decrease in the species concentration boundary layer thickness. This springs from the fact that at high $Sc$, the particles in the fluid concentration are giant with small diffusivity. However, the particles in the fluid concentration are very small with great diffusivity and are scarcely conditioned by the viscosity of the medium in the case of a low $Sc$.

In Table 1, the numerical values of the local Nusselt number in this paper for different values of $\Pr$ and $\alpha$ in the absence of thermal and velocity slip effects without consideration for species concentration in a hydrodynamic flow are in good agreement with the result published in Hayat *et al.* (2011). Therefore, this validates the presented results to be highly accurate to analyze this flow problem. Table 2 presents variations of local skin friction coefficient, Nusselt and Sherwood numbers in relation to $K$, $Mn$, $S$, $\alpha$, $B$, $A$ and $Sc$. From this table, as the values of Deborah number, magnetic interaction, suction, stretching and thermal slip parameters increase, the values of local skin friction coefficient increase. However, the local skin friction coefficient is found to decrease as the value of velocity slip increases. Also, it is worthy to note that as the values of $K$, $Mn$, $\alpha$ and $B$ increase, the local rate of heat transfer decreases whereas an increase in the values of $S$, $A$ and $\Pr$ is found to increase the local heat transfer rate. Finally, it is evident from Table 2 that the local rate of mass transfer is enhanced by increasing the values of Schmidt number, Prandtl number, suction, stretching and thermal slip parameters. In contrast, as the values of Deborah number, magnetic interaction and velocity slip parameters increase, the local Sherwood number decreases.

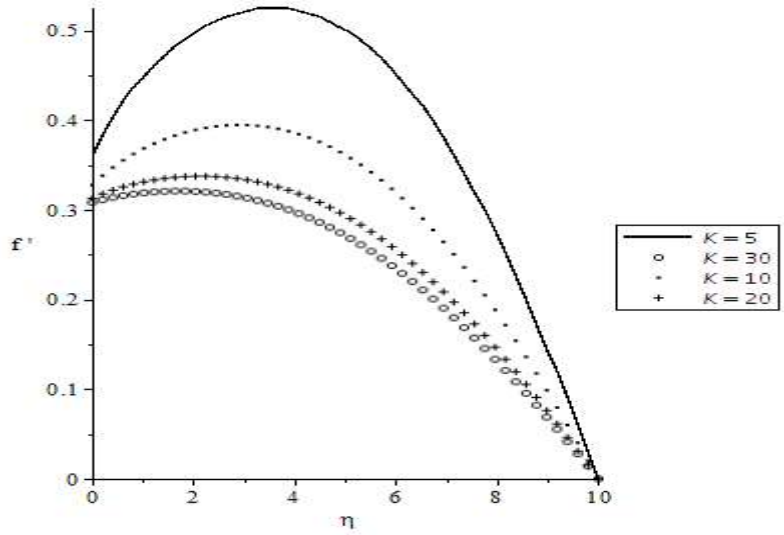


*Fig. 1: Variation of* $K$ *on velocity field when* $Mn = 0.5,\ S = 0.5,\ \alpha = 0.1,\ A = 0.1.$

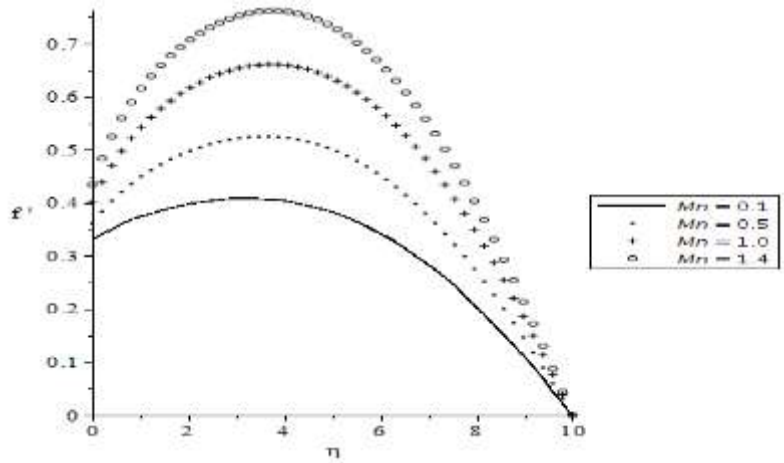


*Fig. 2: Variation of* $Mn$ *on velocity field when* $K = 5,\ S = 0.5,\ \alpha = 0.1,\ A = 0.1.$

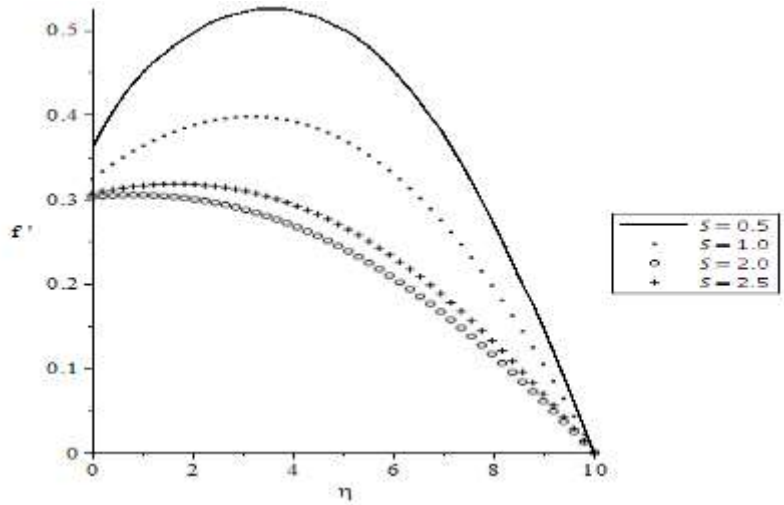


Fig. 3: Variation of $S$ on velocity field when $K = 5,\ Mn = 0.5,\ \alpha = 0.1,\ A = 0.1.$

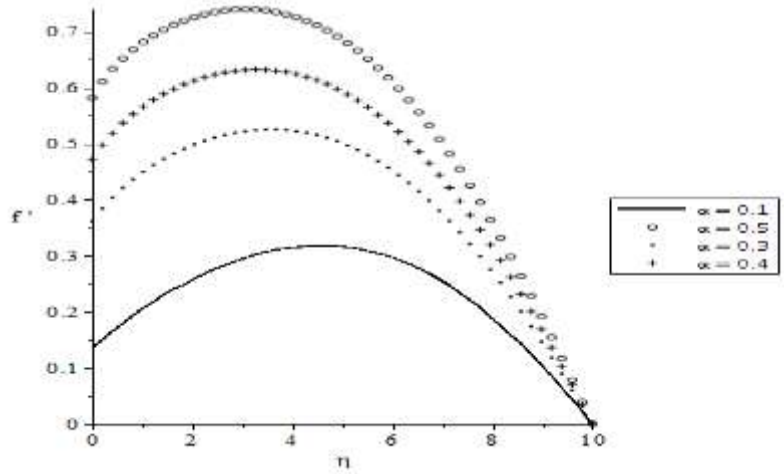


*Fig. 4: Variation of* $\alpha$ *on velocity field when* $K = 5,\ S = 0.5,\ Mn = 0.5,\ A = 0.1.$

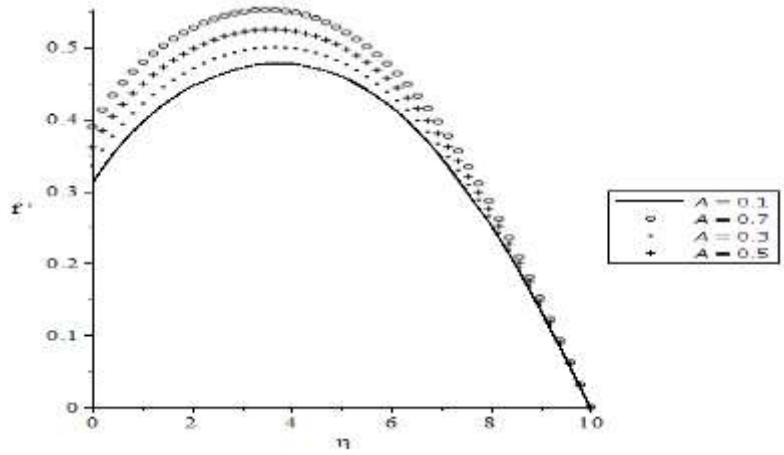


*Fig. 5: Variation of* $A$ *on velocity field when* $K = 5,\ S = 0.5,\ \alpha = 0.1,\ Mn = 0.5.$

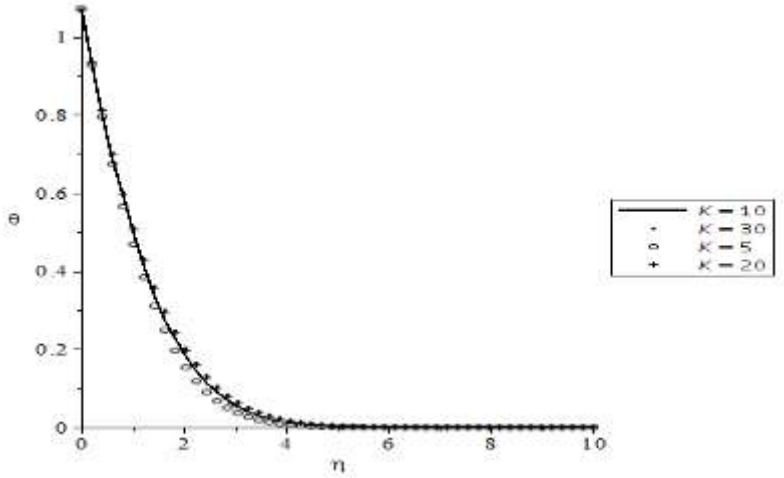


*Fig. 6: Variation of* $K$ *on temperature field when* $\Pr = 0.71,\ B = 0.5,\ S = 0.5.$

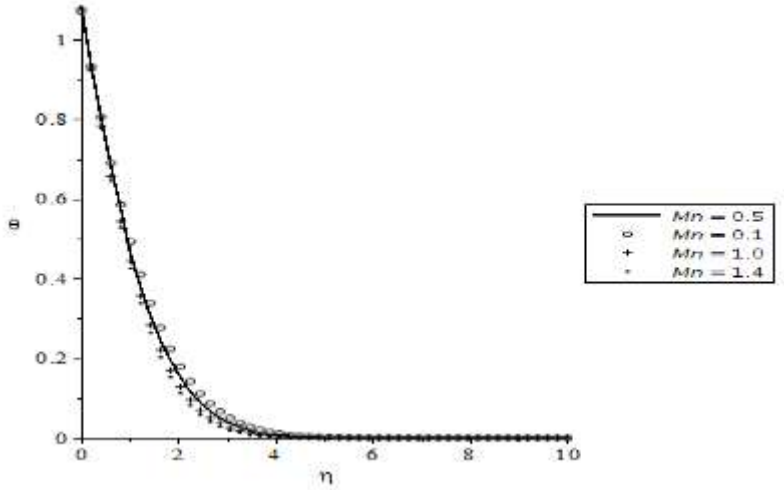


*Fig. 7: Variation of* $Mn$ *on temperature field when* $\Pr = 0.71,\ B = 0.5,\ K = 5,\ S = 0.5.$

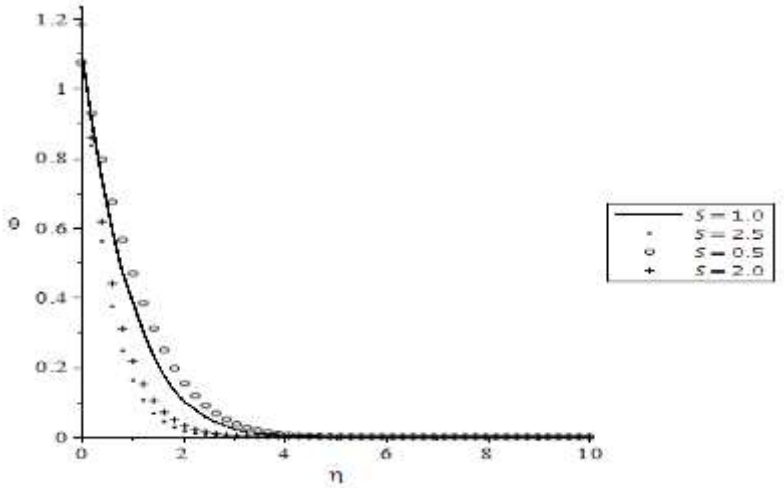


*Fig. 8: Variation of* $S$ *on temperature field when* $\Pr = 0.71,\ B = 0.5,\ K = 5,\ \alpha = 0.5.$

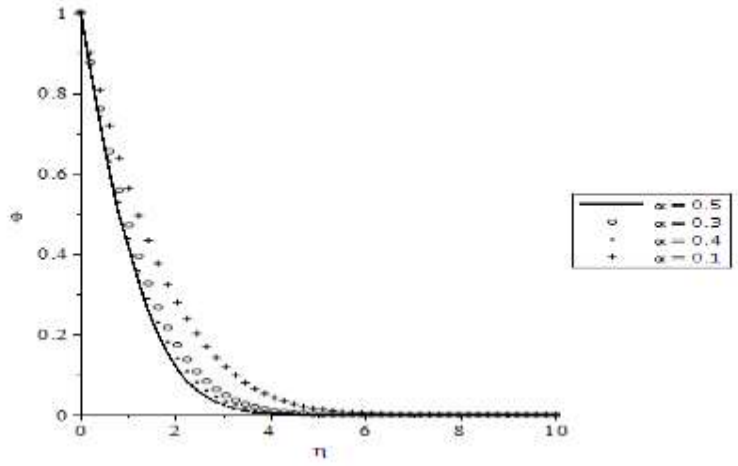


*Fig. 9: Variation of* $\alpha$ *on temperature field when* $\Pr = 0.71,\ B = 0.5,\ K = 5\ \ S = 0.5.$

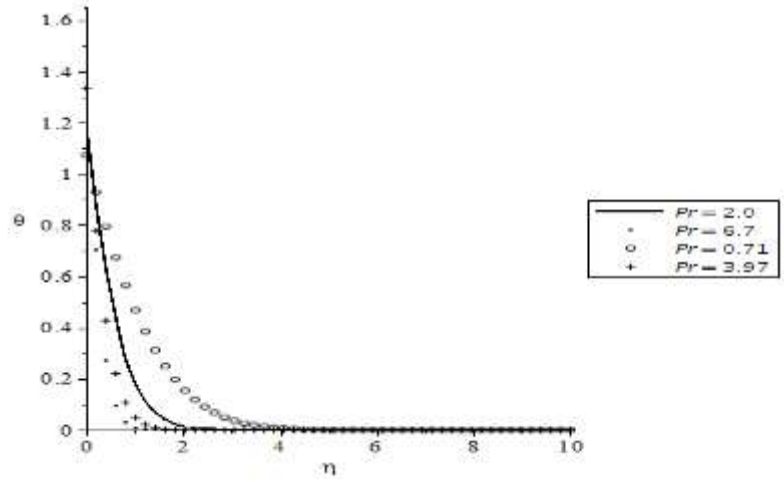


*Fig. 10: Variation of* $\Pr$ *on temperature field when* $\alpha = 0.3,\ B = 0.5,\ K = 5\ \ S = 0.5.$

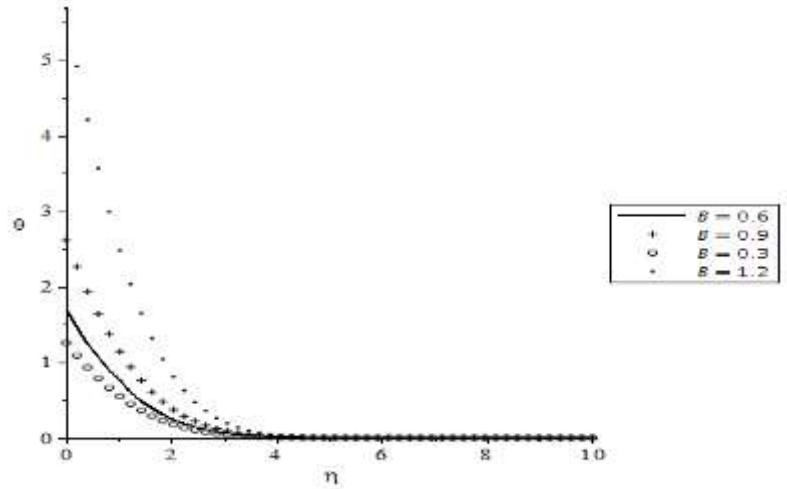


*Fig. 11: Variation of* $B$ *on temperature field when* $\Pr = 0.71,\ \alpha = 0.3,\ K = 5\ \ S = 0.5.$

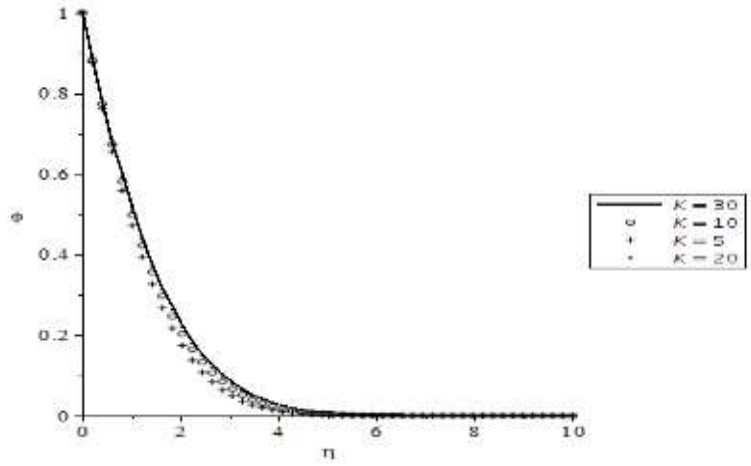


*Fig. 12: Variation of* $K$ *on species concentration field when* $Sc = 0.62,\ A = 0.1,\ \alpha = 0.3.$

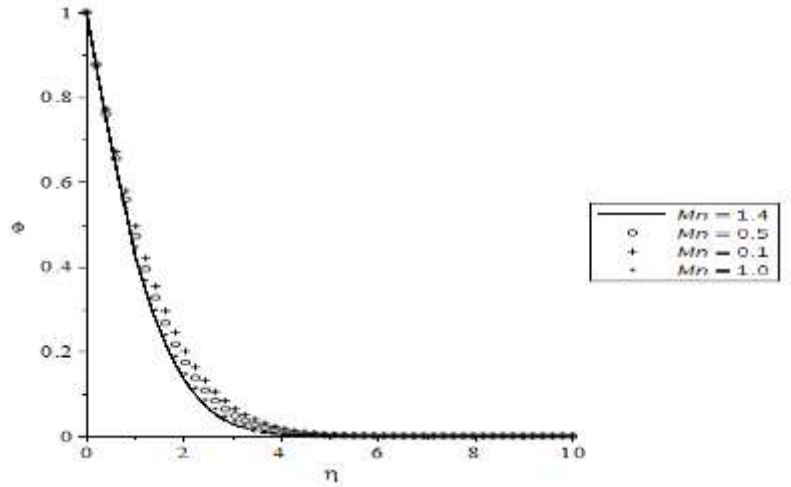


*Fig. 13: Variation of* $Mn$ *on temperature field when* $Sc = 0.62,\ A = 0.1,\ K = 5.$

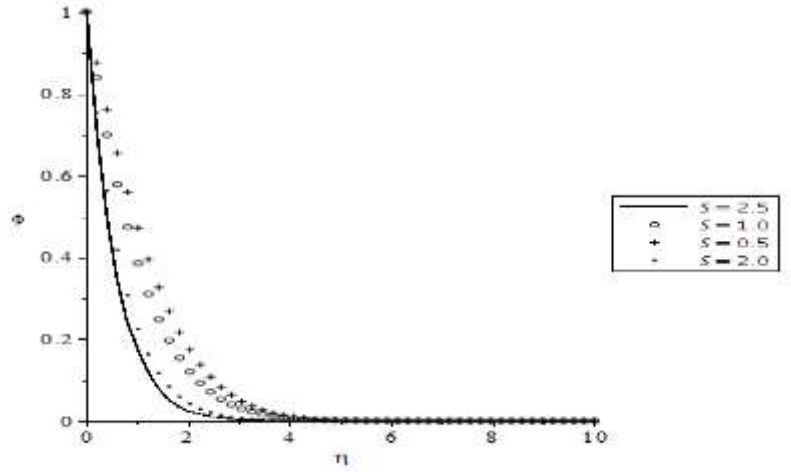


*Fig. 14: Variation of* $S$ *on species concentration field when* $Sc = 0.62,\ A = 0.1,\ K = 5.$

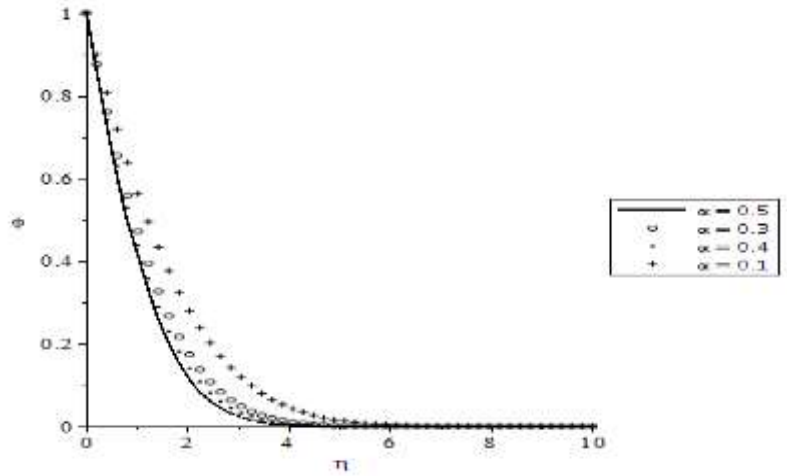


*Fig. 15: Variation of* $\alpha$ *on species concentration field when* $Sc = 0.62,\ A = 0.1,\ K = 5$.

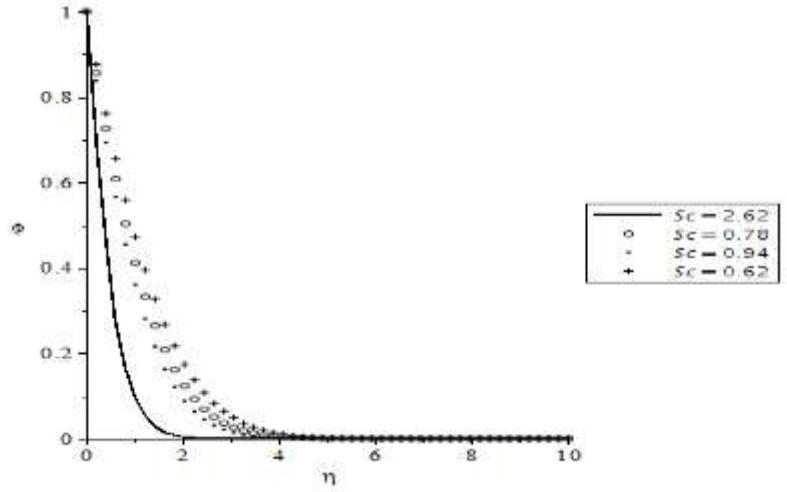


*Fig. 16: Variation of* $Sc$ *on species concentration field when* $\alpha = 0.3,\ A = 0.1,\ K = 5$.

Table 1: Comparison of the values of local Nusselt number $-\theta'(0)$ for parameters $\Pr$ and $\alpha$ when $S = 0.5$, $K = 0.2$, $Mn = A = \phi = Sc = 0.0$ with convective boundary conditions.

| Pr | $\alpha$ | $Nu/\mathrm{Re}_x^{1/2}$ Hayat *et al.* (2011) | $Nu/\mathrm{Re}_x^{1/2}$ (Present Work) |
|---|---|---|---|
| 0.5 | | 0.23336 | 0.23389 |
| 1.0 | | 0.36588 | 0.36625 |
| 1.5 | | 0.45796 | 0.45797 |
| 2.0 | | 0.52558 | 0.52557 |
| 1.0 | 0.1 | 0.36588 | 0.36605 |
| | 0.3 | 0.40466 | 0.40473 |
| | 0.8 | 0.45825 | 0.45830 |
| | 1.0 | 0.47254 | 0.47256 |

Table 2: Values of local skin friction coefficient, Nusselt and Sherwood numbers when $K = 0.1$, $\alpha = 0.4$, $Mn = 5$, $S = 0.5$, $A = 0.3$, $B = 0.5$ :

| $K$ | $Mn$ | $S$ | $\alpha$ | $B$ | $A$ | Pr | $Sc$ | $f''(0)$ | $-\theta'(0)$ | $-\phi'(0)$ |
|---|---|---|---|---|---|---|---|---|---|---|
| 0 | | | | | | | | 0.44748648380 | 1.7171884483 | 0.52650918336 |
| 0.05 | | | | | | | | 0.44924048847 | 1.7168179769 | 0.52587656009 |
| 0.1 | | | | | | | | 0.45101139096 | 1.7164444768 | 0.52524311031 |
| | 3 | | | | | | | 0.40945138478 | 1.7253144609 | 0.54148202163 |
| | 5 | | | | | | | 0.45101139096 | 1.7164444768 | 0.52524311031 |
| | 7 | | | | | | | 0.47921470538 | 1.7105850549 | 0.51586332597 |
| | | 0.4 | | | | | | 0.44556498546 | 1.5497417149 | 0.43771808739 |
| | | 0.6 | | | | | | 0.45670349922 | 1.8556991433 | 0.61439952931 |
| | | 0.8 | | | | | | 0.46888539045 | 2.0743628798 | 0.79509239683 |
| | | | 0.4 | | | | | 0.45101139097 | 2.6136979637 | 0.52524311031 |
| | | | 0.5 | | | | | 0.56491773883 | 1.7266724783 | 0.53739249889 |
| | | | 0.6 | | | | | 0.67927137462 | 1.2888738914 | 0.54931777077 |
| | | | | 0.1 | | | | 0.45101139097 | 2.6136979637 | 0.52524311031 |
| | | | | 0.3 | | | | 0.56491773883 | 1.7266724783 | 0.53739249889 |
| | | | | 0.4 | | | | 0.67927137462 | 1.2888738914 | 0.54931777077 |
| | | | | | 0.6 | | | 0.40500731931 | 0.4736597134 | 0.52025764732 |
| | | | | | 0.9 | | | 0.31027478115 | 1.0750066594 | 0.50984564267 |
| | | | | | 1.3 | | | 0.23663087318 | 1.7317290774 | 0.50161323008 |
| | | | | | | 1 | | 0.45101139025 | 0.4775382556 | 0.52524311020 |
| | | | | | | 5 | | 0.45101139093 | 1.4807989246 | 0.52524311030 |
| | | | | | | 7 | | 0.45101139096 | 1.7517901039 | 0.52524311031 |
| | | | | | | | 1 | 0.45101139097 | 1.7164444768 | 0.55739089901 |
| | | | | | | | 3 | 0.45101139097 | 1.7164444768 | 1.62352126635 |
| | | | | | | | 5 | 0.45101139097 | 1.7164444768 | 2.66445599848 |

## CONCLUDING REMARKS

In this paper, the upper-convected Maxwell model with thermal and velocity slip effects is employed to investigate the heat and mass transfer of Maxwell fluid over stretching sheet in the presence of a transversely applied uniform magnetic field. The numerical results suggest the following:

- The velocity field increases for higher estimation of stretching and magnetic interaction parameters but it decays with increasing values of Deborah number and suction parameter.
- The temperature distribution is enhanced by increasing values of Deborah number and thermal slip parameter. However, the temperature is a decreasing function of Prandtl number, magnetic interaction, suction and stretching parameters.
- The species concentration field increases by increasing values of Deborah number and thermal slip parameter whereas the field is found to decay with increases in the values of Schmidt number, magnetic interaction, suction and stretching parameters.
- The Deborah number, magnetic interaction, stretching, thermal slip and suction parameters have similar effects on the local skin friction coefficient. Local rate of heat transfer decreases with an increase in the values of Deborah number, magnetic interaction, stretching and thermal slip parameters. However, the local rate of mass transfer is an increasing function of the Schmidt number, suction, stretching and thermal slip parameters.

## REFERENCES

Abel, M.S. and Mahesha, N. (2008). Heat transfer in MHD viscoelastic fluid flow over a stretching sheet with variable thermal conductivity, non-uniform heat source and radiation. *Applied Mathematical Modeling, 32: 1965-1983.*

Adegbie, K.S., Omowaye, A.J., Disu, A.B. and Animasaun, I.L. (2015). Heat and mass transfer of upper convected Maxwell fluid flow with variable thermophysical properties over a horizontal melting surface. *Applied Mathematics 6 (08), Article ID:8410.* doi:10.4236/am.2015.68129.

Anderson, H.I. (1992). MHD flow of a viscoelastic fluid past a stretching surface. *Acta Mechanica, 95: 227-230.*

Baoku, I.G. (2014). Effects of suction and thermal radiation on heat transfer in a third grade Fluid over a Vertical Plate. *Physical Science: International Journal, 4(9): 1293 - 1310.*

Baoku, I.G. and Olajuwon, B.I. (2014). Transient flow and mass transfer of a third grade fluid past a vertical porous plate in the presence of chemical reaction. *Nigerian Journal of Science, 48: 47 – 56.*

Baoku, I.G., Onifade, Y.S., Adebayo, L.O. and Yusuff, K.M. (2015). Heat and mass transfer in a second grade fluid over a stretching vertical surface in a porous medium. *International Journal of Applied Mechanics and Engineering, 20(2): 239 – 255.*

Eldabe-Nabil, T.M and Mohammed-Mona, A.A. (2002). Heat and mass transfer in hydromagnetic flow of the non-Newtonian fluid with heat source over an accelerating surface through a porous medium. *Chaos Solutions and Fractals, 13: 907-917.*

Fetecau, C. and Fetecau, C. (2003). Anew solution for the flow of a Maxwell past an insulated plate. i*nternational Journal of Non-Linear Mechanics 38, 423-427.*

Fetecau, C. and Fetecau, C. (2003). Decay of potential vortex in a Maxwell fluid. *International Journal of Non-Linear Mechanics 38, 985-990.*

Fetecau, C. and Fetecau, C. (2003). The Rayleigh Stokes problem for a fluid of Maxwellian type. *International Journal of Non-Linear Mechanics 38, 603-607.*

Gupta, R.K. and Sridhar, T. (1985). Visco-elastic effects in non-Newtonian flow through porous media. *Rheologica Acta 24: 148-151.*

Hayat, T. and Qasim, M. (2010). Influence of thermal radiation and Joule heating on MHD flow of a Maxwell fluid in the presence of thermophoresis. *International Journal of Heat and Mass Transfer,* 53*(21-22):*4780-*4788.* doi:10.1016/j.ijheatmasstransfer.2010.06.014.

Hayat, T. and Sajid, M. (2006). Serial solution for the upper-convected Maxwell fluid over a porous stretching plate. *Physics Letters A,* 358: *396-403.*

Hayat, T. and Sajid, M. (2007). Homotopy analysis of MHD boundary layer flow of an upper convected Maxwell fluid. *International Journal of Engineering Science 45, 393-401.*

Hayat, T., Abbas, Z. and Ali, N. (2008). MHD flow and mass transfer of an upper-convected Maxwell fluid past a porous shrinking sheet with chemical reaction species. *Physics Letters A, 372(26): 4698-4704.* doi:10.1016/j.physleta.2008.05.006.

Hayat, T., Ashraf, B. M., Alsaedi, A. and Shehzad, S. A. (2015). Convective heat and mass transfer effects in three-dimensional flow of Maxwell fluid over a stretching surface with heat source. *Journal of Central South University, 22(2): 717-726.*

Hayat, T., Hina, S. and Hendi, A.A. (2010). Slip effects on the magnetohydrodynamic peristaltic flow of a Maxwell fluid, *Z. Naturforsh. 65a, 1123-1136.*

Hayat, T., Shehzad, S. A., Qasim, M. and Obaidat, S. (2011). Steady flow of Maxwell fluid with convective boundary conditions. *Z. Naturforsch A. 66a, 417-422.*

Heck, A. (2003). *Introduction to Maple,* Third Edition, Springer-Verlag, Germany.

Ishak, N., Hashim, H., Mohamed, M. K. A., Sarif, N.M., Khaled, M., Rosli, N. and Salleh, M.Z. (2015). MHD flow and heat transfer for the upper-convected Maxwell fluid over a stretching/shrinking sheet with prescribed heat flux. *AIP Conference Proceedings 1691 ,040011.* https://doi.org/10.1063/1.4937061.

Khan, S.K. and Sanjayanand, E. (2005). Viscoelastic boundary layer flow and heat transfer over an exponentially stretching sheet. *International Journal of Heat and Mass transfer, 48:1534-1542.* doi10.1016/j.ijheatmasstransfer.2004.10.032.

Koríko, O. K., Adegbie, K. S., Omowaye, A. J. and Animasaun, I.L. (2016). The boundary layer of an Upper- convected Maxwell fluid flow with variable thermo-physical properties over a melting thermally stratified surface. *FUTA Journal of Research in Sciences, 12(2), 287-298.*

Koriko, O.K., Oreyeni, T., Omowaye, A.J. and Animasaun, I.L. (2016). Homotopy analysis of MHD free convective micropoar fluid flow along a vertical surface embedded in non-Darcian thermal-stratified medium, *Open Journal of Fluid Dynamics, 6: 198-221.*

Lin, Y. and Guo, B. (2017). Effect of second-order slip on the flow a fractional Maxwell MHD fluid. *Journal of the Association of Arab Universities for Basic and Applied Sciences 24, 232-241.*

Mushtaq, A., Mustafa, M., Hayat, T. and Alsaedi, A. (2014). Effects of thermal radiation on the stagnation-point flow of upper-convected Maxwell fluid over a stretching sheet. *Journal of Aerospace Engineering 27(4), 04014015.* doi:10.1061/(ASCE)AS.1943-5525.0000361.

Mustafa, M., Khan, J.A., Hayat, T. and Alsaedi, A. (2015). Simulations for Maxwell fluid flow past a convectively heated exponentially stretching sheet with nanoparticles. *AIP Advances5, 037133.* https://doi.org/10.1063/1.4916364.

Olajuwon, B.I. and Baoku, I.G. (2014). Numerical study of heat and mass transfer in a transient third grade fluid flow in the presence of heat source, chemical reaction and thermal radiation. *Daffodil International University Journal of Science and Technology, 9(2): 25 - 36.*

Omowaye, A.J. and Animasaun, I.K. (2016). Upper-convected Maxwell fluid flow in variable thermophysical properties over a melting surface situated in hot environment subject to thermal stratification. *Journal of Applied Fluid Mechanics 9(4), 1777-1790.*

Pop, I., Sujatha, A., Vajravelu, K. and Prasad, K.V. (2012) MHD Flow and Heat Transfer of a UCM Fluid over a Stretching Surface with Variable Thermophysical Properties. *Meccanica, 47, 1425-1439.* http://dx.doi.org/10.1007/s11012-011-9526-x

Popoola, A. A., Baoku, I. G. and Olajuwon, B. I. (2016).Heat and mass transfer on MHD viscoelastic fluid flow in the presence of thermal diffusion and chemical reaction. *Journal of Heat and Technology, 34: 15 - 26.*

Prasad, K.V., Dulal, P., Umesh, V. and Prasanna Rao, N.S. (2010). The effect of variable viscosity on a MHD viscoelastic fluid flow and heat transfer on a stretching sheet. *Communication in Nonlinear Science and Numerical Simulation, 15: 331-344.*

Rahbari, A., Abbasi, M., Rahimipetroudi, I., Sundén, B., Domiri G. D., and Gholami, M. (2018). Heat transfer and MHD flow of non-Newtonian Maxwell fluid through a parallel plate channel: analytical and

numerical solution. *Mechanical Sciences 9: 61-70.* https://doi.org/10.5194/ms-9-61-2018.

Sadeghy, K, Najafi, A.H. and Saffaripour, M. (2005). Sakiadis flow of an upper-convected Maxwell fluid. *International Journal of Non-Linear Mechanics 40: 1220-1228.*

Sajid, M., Abbas, Z., Ali, N., Javed,T. and Ahmad, I. (2014). Slip flow of a Maxwell fluid past a stretching sheet. *Walailak Journal of Science and Technology, 11(12), 1093- 1103.*

Sajid, M., Awais, M., Nadeem, S. and Hayat, T. (2008). The influence of slip condition on thin film flow of a fourth grade fluid by the homotopy analysis method. *Computers and Mathematics with Applications, 56, 2019-2026.*

Sanjayanand, E. and Khan, S.K. (2006). On heat and mass transfer in a viscoelastic boundary layer flow over an exponentially stretching sheet. *International Journal of Thermal Science, 45: 819-828.*

Sarpakaya, T. (1961). Flow of non-Newtonian fluids in a magnetic field. *AlChE Journal, 7: 324-328.*

Shateyi, S., Motsa, S.S. and Makukula, Z. (2015). On spectral relaxation method for entropy generation in a MHD flow and heat transfer of a Maxwell fluid. *Journal of Applied Fluid Mechanics, 8 (1), 21-31.*

Soundalgekar, V.M. (1974). Stokes problem for elastico-viscous fluid. *Rheologica Acta, 13:744-746.*

Vajravelu, K. and Rollins, D. (2004). Hydromagnetic flow of a second grade fluid over a stretching sheet. *Applied Mathematics and Computation, 148: 783-791.*

Vieru, D. and Zafar, A. A. (2013). Some Couette flows of a Maxwell fluid with wall slip condition. *Applied Mathematics and Information Sciences: An International Journal, 7(1), 209-219.*

Wang, S.W. and Tan, W.C. (2008). Stability analysis of double-diffusive convection of Maxwell fluid in a porous medium heated from below. *Physics Letter A, 372: 3046-3050.*

Zierep, J. and Fetecau, C. (2007). Energetic balance for the Rayleigh-Stokes problem of a Maxwell fluid. *International Journal of Engineering Science, 45(2): 617-627.*